RSC Advances

ROYAL SOCIETY OF CHEMISTRY

www.rsc.org/advances

Minerals Substituted Hydroxyapatite Coatings Deposited on TiO_2 Nanoporous Modulate the Directional Growth and Activity of Osteoblastic Cells†

Dharman Govindaraj,[a] Mariappan Rajan,[a]* Murugan A. Munusamy[b], and Akon Higuchi[b, c]

[a]*Department Of Natural Products Chemistry, School of Chemistry, Madurai Kamaraj University, Madurai 625021, India.*Phone: +91 9488014084. E-mail Id: rajanm153@gmail.com*

[b]*Department of Botany and Microbiology, College of Science, King Saud University, Riyadh, Kingdom of Saudi Arabia.*

[c]*Department of Chemical & Materials Engineering National Central University ,No. 300 Jung da Rd., Chung-Li, Taoyuan 320, Taiwan, R.O.C.*

Abstract

The biocompatibility of anodized titanium (TiO_2) was improved by an electrophoretically deposited minerals (strontium (Sr), magnesium (Mg) and zinc (Zn)) substituted hydroxyapatite (M-HAP). The M-HAP layer was grown on the anodized Ti surface with different deposition temperature (room temperature, 60 and 80^oC). The phases and morphologies for the M-HAP layers were influenced by the deposition temperature. The coatings characterize by Fourier transform infrared spectroscopy (FT-IR), X-ray diffraction (XRD), X-ray photoelectron spectroscopy (XPS), Scanning electron microscopy equipped with energy dispersive X-ray analysis (SEM-EDX). Also, the effects of temperature and the minerals substitution of Sr, Mg and Zn for Ca on the physiochemical and biological properties of the M-HAP coatings were evaluated by the mechanical strength, ion dissolution and proliferation, alkaline phosphatase (ALP) activity and osteogenic expression of osteoblast like cells MG66 (HOS). Thus, the M-HAP deposition of TiO_2 will serve as a potential candidate for orthopedic applications.

1. Introduction

Commercially pristine titanium and its alloys are extensively applied in the study of biomedical implants, for example, dental and orthopaedic implants and the bio-compatibility of the titanium surface has been attributed to its firm oxide.[1] In addition, surface alteration is used to regulate the properties of the titanium implant for specific medical applications, but there are still disadvantages of pristine Ti and its alloys.[2] One of the most significant ones with these problems is stress shielding that commonly comes up because of the high rigidity and bio-inertness of Ti and its alloys compared to bone tissue which, in elongated times, results in poor or inadequate adhesion between bone-implant contact under *invivo* conditions.[3] The long-term survival of these Ti implants is additionally dependent on existing of bacteria surrounding the implants.[4] Pure Ti exhibits poor antibacterial activity.[5] The conclusion of such problems would be implanted loosening and consequent demand for re-operation.

To overcome these obstacles, to increase the bioactivity, osteointegration and antibacterial activity of the implants, an extensive range of technologies had been existing to alter the surface properties to specific requirements.[6] Such treatments include anodization[7] and deposition with hydroxyapatite (HAP).[8]

An increasing number of data declare the benefits of nanoporous TiO_2 in numerous medical fields, especially orthopedic.[9] The nanoporous TiO_2 were likewise used for increase orthopedic implant surfaces and increase the formation of HAP.[10] HAP ($Ca_{10}(PO_4)_6(OH)_2$), the main inorganic composition in normal bone, was extensively used as coating bio-ceramic for biomedical applications.[11-12] However, the effective use of HAP has a few disadvantages which additionally include with absence of antibacterial activity that too affects its long-term stability and gives elevated to implant failures.[13]Furthermore, to develop deposition features, such as

osteointegration, antibacterial activity and bio-activity, HAP bio-ceramics can be substituted with small amounts of ions that are found in natural bones and tooth mineral.[14] It is evidenced that hydroxyapatite structure has immense flexibility in patient substitution. The addition of minute quantities of ions such as Mg, Mn, Sr and Zn addicted to HAP structure improves the biological properties of HAP.[15] Consequently, the ionic inclusion such as magnesium (Mg), strontium (Sr) and zinc (Zn) into HAP bio-ceramics has been of huge attention for biological process after implantation. Magnesium assumes an imperative part in anticipating osteoporosis in human bone.[16] Strontium is a bone-seeking for component that shows helpful impact on bone growth.[17]Zinc also has the stimulatory effect on bone formation *in vivo*. [18]

In this way Sr^{2+}, Mg^{2+} and Zn^{2+} as vital elements, were found to be exceptionally successful in improving the structural steadiness and biological properties of apatite. Both *in vivo* and *in vitro* studies have additionally obviously showed that Sr^{2+}, Mg^{2+} and Zn^{2+} influence the mineral metabolism during the osseous tissue remodelling process and enhance pre osteoblastic cell multiplication.[19]

To the best of our knowledge, there are no reports of mineral substituted hydroxyapatite electrophoretic deposition of anodized titanium for biomedical applications. In this report, we have described the successfully fabricated minerals substituted hydroxyapatite (M-HAP) electrophoretically deposited (EPD) on TiO_2 under different temperature (Room temperature, 60 and $80^{O}C$). Moreover, the deposition layers were characterized in terms of morphology, crystallinity change, and adherence properties. The antibacterial efficiency of the deposited M-HAP on TiO_2 was determined using S. aureus. This study also investigated cytocompatibility and cell proliferation of the deposited M-HAP on TiO_2 by using cells of the human osteosarcoma cell (HOS) MG63. All these observations recommend that the M-HAP/TiO_2 is going to promising

implant for orthopaedic/dental biomaterials engineering applications**.**

2. Experimental Sections

2.1. Materials and methods

Experiments were conducted on 0.25 mm thick pristine titanium foils (99.7% purity, Sigma Aldrich) were employed as substrate along with phosphoric acid 99% (Sigma Aldrich) and ammonium fluoride 99% (Merck) as initial materials for anodizing scheme. The hydroxyapatite and minerals substituted hydroxyapatite with particle size between 50 and 100 nm synthesized by microwave method (reported in the Supplementary experimental Section, Figure. S4), together with n-butanol (Sigma Aldrich) and triethanolamine solutions were subject to run electrophoretic deposition process. Hydrogen fluoride (HF) 48% (Sigma Aldrich) and H_3PO_4 99% (Merck) solutions were used for chemical cleaning of titanium foils earlier to anodizing achieve. Two procedures were followed in regulate to form nanoporous TiO_2 depositions containing M-HAP, namely (I) Anodizing method in order to fabricate TiO_2 nanoporous structures and (II) Electrophoretic deposition of M-HAP onto TiO_2 under different temperature.

2.2. Synthesis of titanium nanoporous

Formation of nanoporous TiO_2 structures pristine titanium foils were ultrasonically cleaned (EN-60US (Microplus) at the frequency of 28 kHz and 150 W) through acetone, 2-propanol and ethanol, followed by chemical clean-up in H_3PO_4/HF solution. Then, nanoporous TiO_2 were engendered by anodization of Ti foils in 300 ml of an electrolytic solution utilizing ultrasonic waves (EN-60US (Microplus) at the frequency of 28 kHz and 150 W). A direct current (Aplab High Voltage, DC Power Supply H0310,15 - 300 V DC and 1 A Max) power source was subsidiary to the operation of electrochemical anodization. The Titanium foils were

subjected to anodizing development in a two-electrode cell filled with a fluorine solution composed of 1 M H_3PO_4+ 0.8 wt% NH_4F in which Ti foil and a Platinum mesh were used as the anode and cathode of the cell, respectively. Anodizing potential of the cell was set at 30V. The anodic oxidation progression was carried out for 5h at room temperature.

2.3. Suspension preparation

Suspensions were prepared by adding 0.6 g minerals superseded hydroxyapatite (M-HAP) powder to 100 mL n-butanol. Following magnetically stirring for 12 h, suspensions were dispersed ultrasonically for 20 min used (EN-60US (Microplus) at the frequency of 28 kHz and 150 W) to ensure a fine dispersion. Subsequent to 10 min of being left at ambient temperature for cooling, the suspension was prepared for running the EPD process.

2.4. EPD

In the succession to form electrophoretically deposited M-HAP nanoparticles on the nanoporous TiO_2 substrate, an electrophoretic cell was situated with nanoporous TiO_2 substrate (resulting from anodization processes) as the cathode and pristine titanium sheets as anode. The EPD process was transmitted at 120 V for 3 min and at different temperature (room temperature, 60 and 80^{O}C). Then, coated samples were dried at room temperature in still air for 12 h, and determinately sintered at the 400 ^{O}C in an argon atmosphere. The pure HAP was also coated by the same process.

2. 5. Morphology and phase analysis

2.5.1. X-ray diffraction (XRD)

A Bruker D8 advanced XRD instrument was working for the phase identification and the crystallinity of the M-HAP depositions. Designed for the XRD experiments, Cu Kα incident radiation, a tube voltage of 40 kV and a current of 30 mA was used and the scanning angle is

ranged from 20 to 60°, with a scan rate (2θ) of 0.02°.

2.5.2. Scanning electron microscopy (SEM)–energy-dispersive spectroscopy (EDS)

The surface morphology and elemental composition of the composite deposition were examined using SEM (SEM-JEOL JSM-6400, Japan) equipped with EDX analysis.

2.5.3. Fourier transforms infrared spectroscopy tests

Fourier transform infrared (FTIR) spectroscopic studies (Nicolet 380, Perkin Elmer, USA) were carried out to identified compositional characteristics of the coatings.

2.5.4. XPS characterization

X-ray photoelectron spectroscopy (XPS) was habituated to evaluate the elemental composition of the M-HAP on TiO_2 deposition. The XPS spectra were proceedings by an SSX-100 spectrometer with monochromatised X-ray Al Kα radiation (1486.6 eV). The resolution was calculated as plenary width at half maximum of 1.0 (core-level spectrum) to 1.5 eV.

2.5.5. Ionic release measurement

The coated disks were immersed in 10 ml of stimulated body fluid solution (SBF) in a preserved bottle at 37^{o}C for 1, 3, and 7 days, with mild shaking. After immersion, the concentrations of Ti, Ca, Mg, Sr, Zn and P ions released from the samples into the solution were measured by ICP-AES (Thermo Jarrel Ash-Atom Scan (USA). Measurements were performed three times for every drenching time point, and tests were run in triplicate.

2.5.6. Adhesion properties

The bond strength of the M-HAP deposited on TiO_2 was evaluated by pull-out test according to the American Society for Testing Materials (ASTM) international standard F1044-05.[20] With five experiments for all sample was carried out. The specimens were subjected to tests at a steady cross-head speed utilizing a macrocosmic testing machine (Model 5569, Instron).

2.6. Biological characterizations of the coatings

2.6.1. Antibacterial activity

The convention of antibacterial rates concerning planktonic bacteria in the culture medium (Rp) and the antibacterial rates for adhered bacteria on the specimens (Ra) were calculated based on Zhao et al., reported method.[21] Antibacterial action was assessed using Staphylococcus aureus (ATCC 25923) developed in a beef extract-peptone (BEP) medium at 37^{o}C for 12 h and adjusted to a concentration of 10^5 CFU/mL. Each specimen was incubated in 1mL of bacterial suspension at 37^{o}C for 1 day. Following the incubation period, the culture medium was sampled to determine the viable counts of planktonic bacteria. The specimens were delicately flushed with PBS three times to eliminate non-adherent bacteria, and the adherent bacteria on each specimen were isolates into 1 mL of BEP by sonication at 50 W for 2min. The subsequent bacterial suspension was sampled to count the viable bacteria adhered to the specimens. Afterwards, the specimens were ultrasonically cleaned, dried, sterilized, and re-incubated as described above. This process was rehashed day by day for a total incubation time of 7 days. The viable bacteria in the sampled suspensions on days 1, 3 and 7 were counted by serial dilution using the spread plate method.

2.6.2. Cell culture

The biocompatibility of M-HAP deposition was evaluated by culturing Human osteosarcoma HOS MG63 cells obtained from National Centre for Cell Science (NCCS), Pune, India were cultured in minimal essential media (Hi Media Laboratories) supplemented with 10% Fetal Bovine Serum, Streptomycin (100 U/ml) and Penicillin (100U/ml). The medium was refreshed every 2 days. The cell culture was then incubated below the humidified atmosphere (CO_2) at 37 °C. The samples under examinations were sterilised in an autoclave at 120 °C during 2 h and

placed in 24 well cell culture plates.

2.6.3. Cytotoxicity

The culture medium was removed from each culture well after 1, 3 and 7 days of incubation, and the samples were then transferred to new 24-cell culture plates at a density of $2x10^4$ cells per well. Then, the cells were incubated with a tetrazolium salt solution, 3-[4,5-dimethylthiozol-2-yl]-2, 5-diphenyltetrazolium bromide (MTT) 10 mg/ml for 4 h, and then the MTT solution was detached. After that, the dimethylsulfoxide (DMSO) 10 % (200 micro litre) was added into all well. The cell viability was evaluated at 570 nm on a spectrophotometric microplate reader. The proliferation rate of cells was quantified by measuring the optical density (OD). Cell viability (%) related to the control wells containing cell culture medium without the samples was calculated based on the standard of five replicates using the subsequent equation:

$$\% \text{ Cell viability} = [A] \text{ test} / [A] \text{ control} \times 100.$$

2.6.4. ALP activity

A one mL cell suspension was seeded onto each specimen and placed in a 24-well plate at a density of $4x10^4$ cells per well. After culturing for 7 days, the cells were washed with PBS and lysed in 0.1 vol % Triton X-100 using the standard freeze–thaw cycles. The ALP activity in the lysis was determined using a colourimetric assay using an ALP reagent containing ap-nitrophenyl phosphate substrate. The absorbance of p-nitrophenol was measured at 405 nm using a microplate reader.

2.6.5. Filopodia extension and morphology

MG63 (HOS) were cultured on HAP/TiO_2, M-HAP/Ti and M-HAP/TiO_2 coated surfaces for 4 h. Cells were then fixed using 4% paraformaldehyde (PFA) in PBS, and permeabilized with 0.1% Triton-X 100 in PBS for 5 min. Samples were blocked using 3% bovine albumin (BSA) in PBS

for 30 min. The surfaces were rinsed three times with PBS and then incubated for 1.5 h with Alexa Fluor 488-conjugated goat anti-mouse IgG secondary antibody (1:200 dilution in 3% BSA in PBS,) for image of rhodamine conjugated phalloidin (1:100 dilution in 3% BSA in PBS, Cytoskeleton) for image of filamentous actin (F-actin). Nuclei were counterstained using Vectashield Mounting Medium (Vector Labs, Burlingame, CA) containing 4 0,6 diamidino-2-phenylindole (DAPI).

Images were captured using fluorescence microscope (Carl Zeiss, Jena, Germany) and Axio imager software. Osteoblast attachment was determined on each surface by evaluating the total number of nuclei visible from 10 non-overlapping fields of view, selected at random. For quantification of cell diffusion, the planar area of cells was measured using AxioVision Software Release 4.8.0.0. The average cell planar area was determined from 10 cells on each sample. To assess the number of focal adhesions. The average number of focal adhesions per cell was determined from 10 cells on each sample by an impartial, blinded observer.

2.6.6. Osteogenesis-related gene expressions

The osteogenic differentiation of MG63 (HOS) cells on the HAP/TiO_2, M-HAP/Ti and M-HAP/TiO_2 coated surfaces was further assessed by quantitative reverse transcription polymerase chain reaction (qRT-PCR) to measure the mRNA expression of genes, including ALP, osteocalcin (OCN), osteoprotegerin (OPG), and type-1 collagen (Col-1) was performed using the Bio-rad MyiQ2 with the Trans Start Top Green qPCR SuperMix (Transgen). Cells were seeded at a density of $4x10^4$ cells per well, cultured for 2 weeks, and then lysized using TRIzol (Invitrogen) to extract RNA (Ribonucleic Acid). Cells from four samples in each group were lysized to obtain sufficient RNA; 1 mg of RNA was then reverse transcribed into complementary DNA (cDNA) using the Superscript II first-strand cDNA synthesis kit (Thermo). The primers for

the target genes are listed in Table I. The expression levels of the target genes were normalized to that of the housekeeping gene beta-actin.

3. Results and Discussion

3.1. Characteristics of anodic TiO_2 nanopores

The SEM morphologies of (a) untreated Ti foil and (b) anodized Ti foil was shown in Figure.1. Following anodization treatment of Ti foil surfaces at 30 V, TiO_2 porous layers were engendered on these surfaces Figure.1 (b). It can be seen that the nanoporous exhibit smooth and even morphology. This nanoporous structure is anticipated to develop bonding and adhesion of electrophoretic deposited M-HAP deposition due to the improved mechanical interlocking. In Figure.1 (c), the XRD pattern for the Ti surface shows only α-Ti peaks. In contrast, the XRD pattern for the anodized Ti surface has peaks for both α-Ti and the TiO_2 phase, the concluding providing evidence of the oxide layer on the Ti surface.[22]

3.2. SEM observation of the M-HAP Deposition

SEM images clearly show that the deposition temperature plays an important part in the mastery of morphology of the depositions.[23] It is likewise considered that high temperature can sustain the coating of HAP on the surface due to high diffusion rate. From on this, the electrophoretic deposition of M-HAP on TiO_2 was performed at room temperature and withal by increasing the temperature to 60 and 80°C. From figure 2 (a) shows create non-uniform large aggregates of irregularly shaped pure HAP nanoparticles on TiO_2 deposited at 80°C. The porous like structured M-HAP is obtained on untreated Ti foil at 80°C (Figure. 2 (b)). The M-HAP deposition on TiO_2 obtained at room temperature (Figure. 2 (c)) exhibited nano-rods like morphology when compared with those of M-HAP deposition on TiO_2 (Figure. 2 (d-e)) obtained nano-whiskers (at 60°C) and nano-flaks (at 80°C) respectively. The elemental composition of HAP deposition on

TiO_2 obtained at 80 °C was investigated by EDX analysis (Figure. 2 (f)).

This SEM investigation demonstrated that as the M-HAP as the deposition temperature rises, differently structured M-HAP was obtained. Previously many research groups reported that the deposition temperature up to 37°C is required to obtain crystalline HAP films [24-26].These electrophoretic deposition process of HAP coating with increasing deposition temperature can be explained by three factors. First, the solubility HA decreases with increasing temperature [27]. Second, a higher deposition temperature encourages the deposition of more crystalline film (It clearly discussed blow (Figure. 5 (a-d).)). Third, Most significantly, as the temperature increased, fewer hydrogen bubbles were found to attach to metal surface, So HAP film was less damaged (It clearly discussed in (Figure. 2 (a-e) & Figure. S2). A possible explanation for attachment of fewer hydrogen bubbles is that they are held on the substrate surface by surface tension, and this force decreases with increasing temperature.[28]

Figure 3 (a) shows the cross-section SEM image of the M-HAP coating at shows its thickness to be about 24.6 ±1.2 μm. The elemental composition of M-HAP deposition on TiO_2 obtained at 80°C was investigated by EDX analysis (Figure. 3 (b)). The intense peak of Ca, Sr, Mg, Zn, P, O and Ti confirms the deposition of M-HAP. Therefore; this deposited layer is believed to be good structures for cell proliferation due to the presence of minerals in HAP.

3.3. FTIR Spectra

The structure of anodized Ti and coated M-HAP was examined by FTIR spectroscopic method. Figure. 4 (a-d) illustrates the FTIR spectra of anodized Ti, M-HAP deposited on TiO_2 under different temperature. In figure 4 (a-d), peaks at 1400 cm^{-1}, this can be assigned to the vibrations of Ti-O bonds of TiO_2 nanoporous.[25] The M-HAP deposited on the TiO_2 samples show P–O bands in 1035 and 962 cm^{-1}.[26] The intensity of these P–O bands enlarged after the electrophoretic deposition conditions, signifying formation of M-HAP on the TiO_2 surface. In

summation, the FTIR spectra of the M-HAP layers in (Figure. 4 (b-d)) have comparable peaks, despite the various conditions of deposition. The FTIR peaks for HPO_4^{2-}, PO_4^{3-}, H_2O, and OH^- can be prognosticable and the peaks among from 1100 to 1033 cm^{-1} are cognate to PO_4^{3-} ions.[27] The FTIR analysis suggested the success of the deposition of M-HAP coatings.

3.4. XRD studies of the depositions

The XRD patterns of the M-HAP layer on TiO_2 are revealed in Figure. 5 (a-d). The major diffraction peaks for HAP are observed 2θ values of 25.9°, 31.7°, 32.2° and 32.9°.[28] While for the M-HAP deposition, the 2θ values experienced a minor shift which might have aroused due to substitution of mineral ions in HAP.[29]From figure 5 (a) it could be observed that the peaks were sharp and intense, which is a better sign of the crystalline nature of the obtained M-HAP deposition on untreated Ti at 80°C. For the XRD patterns of M-HAP composite deposition obtained at room temperature, 60 and 80°C, high intense diffraction peak. The peaks (Figure. 5 (b-d)) also become sharper and intense, which is a clear designation that the crystallinity. Thus, as the temperature is increased, the M-HAP depositions exhibited increased crystallinity. Hence, from this XRD pattern it could be concluded that, the electrophoretic deposition temperature plays an important part in the mastery of phase of the M-HAP depositions with desired crystallinity, which might be suitable for tissue biocompatibility.

3.5. XPS Characterization

XPS is an important surface analytical method, which is auxiliary for the finding of elements present in the M-HAP composite. It also gives precious information of the stoichiometric of the constituent elements in the M-HAP composite. A characteristic survey XPS spectrum from M-HAP/TiO_2 is shown in Figure. 6. The investigation spectrum apperceived Ca, P, Sr, Mg and Zn as the main constituents of the M-HAP deposition on anodized Ti substrate. The observed peak positions proximate to 348.6 and 352.9 eV are accredited to $Ca_2p3/2$ and $Ca_2p1/2$.[34]The apexes

of P2s is 192.4 eV and the peak at 133.4 eV is an overlie of Sr3d and P2p because the Sr3d5/2 (133 ± 0.5 eV), furthermore the P2p (133-134 eV) lines were closely situated to the strontium peak.[34] The peaks of O1s may occur owing to the presence of M-HAP, TiO_2 layer produced during the surface anodization of the Ti substrate, carbonate and absorbed water. The achieved spectra of O1s with a binding energy of 530.8, 531.6 and 532.2 eV are accredited to OH^-, CO_3^{2-} and absorbed H_2O.[34, 35] The peak at 49.9 eV is identified for magnesium[36] and the characteristic binding energy of Zn2p is 1022.5 eV analogous to Zn^{2+} is 1022.4 eV.[37] $Ti2p_{3/2}$ at 458.6 eV and $Ti2p_{1/2}$ at 464.2 eV is the binding energy of titanium dioxide (TiO_2).[38]Thus, the XPS data clearly attests the M-HAP layer deposited on TiO_2, which agree with the FTIR and XRD analyses results.

3.6. Ions released test

In figure S1 shows the concentrations of Ca, P, Sr, Mg and Zn ions released from M-HAP/TiO_2 (at 80^oC) sample into physiological stimulated body fluid solution. After 1to7 days of immersion, no release of Ti ions was detected from all types of samples. In M-HAP nanoparticles, Sr, Mg and Zn ions substitute the Ca position and locate in the crystal structure Therefore, the slow and sustained Sr, Mg and Zn ions release behaviour originates from the slow dissolution of the M-HAP phase of the layer. This kind of release behaviour is propitious for the pharmacological performance of Sr, Mg and Zn ions on the surrounding cells and tissues. In addition to the Sr, Mg and Zn ions release, the dissolution of M-HAP after implantation can cause an increase in the local concentrations of calcium and phosphate ions, thereby facilitating the subsequent mineralization process, which is a crucial step in the bone formation process. It clearly discussed blow (Figure. 7 and 8).

3.7. Adhesion Strength

In figure S2 shows the adhesive strength of the M-HAP deposited on untreated Ti foil was measured as 20.08 ± 0.6 MPa. However, there is a consequential improvement in the adhesion strength of M-HAP deposited on TiO_2 at room temperature, 60 and 80^oC (27.04 ± 0.4 MPa, 29.08 ± 0.9 MPa and 31.06 ± 0.4 MPa) which is even higher than the adhesion strength of HA (7.40 MPa)[39] and M-HAP deposition on untreated Ti foil substrate. Moreover, the anodization treatment and deposition temperature improves the bond strength between the M-HAP deposited layers on TiO_2.

3.8. *In vitro* biological studies of the coating

3.8. 1. Antimicrobial Studies

The antibacterial action against planktonic bacteria in the medium (Rp) and antibacterial rates for adherent bacteria on specimens (Ra) after 7 days were evaluated, and the results are shown in Figure S3(A,B), respectively. The HAP/TiO_2 had an Rp value ranging from 10% to 30%, which was constant with time. Compared with the M-HAP/Ti, the M-HAP/TiO_2 samples had higher Rp values, especially during the week. The Rp values of the HAP/TiO_2 samples decreased with time. At day 7, the Rp values of M-HAP/Ti and M-HAP/TiO_2 were equal to those at day 10 but still higher than that of HAP/TiO_2. The Rp values were greatest for M-HAP/TiO_2, followed by M-HAP/Ti, which had an Rp value greater than that of HAP/TiO_2. Minerals (Sr, Mg and Zn) incorporation was effective in preventing bacterial colonization on specimens during the weeks, as shown in Figure S3(B). On day 1, the Ra value of M-HAP/TiO_2 was almost 100%, and that of M-HAP/Ti was nearly 80%. These values then decreased with time; however, in the 3days, the Ra values of M-HAP/Ti and M-HAP/TiO_2 were greater than 50% and 80%, respectively. In the following week, the samples showed Ra values of<60%.

3.8.2. MTT assay

The biocompatibility of cells on the samples was analysis for 1, 3 and 7 days of incubation, established on the absorbance value from MTT assay to verify the biocompatibility of the deposition. The results are obtainable as a bar diagram in Figure. 8 (e) and the optical images of the viable cells after 7 days of incubation are presented in Figure.7 a-g. Reasonably, the cell number in untreated Ti and TiO_2 foil was considerably lower than those on the coated specimens which is an indication that the M-HAP deposited on TiO_2 exhibit higher biocompatibility than a TiO_2, HAP/TiO_2, and M-HAP/Ti. These results suggest that the nano-rods, nano-whisker and nano-flake morphologies of the electrophoretic deposited M-HAP on TiO_2 afford beneficial environments for cell growth and bone formation. This M-HAP deposited surface on TiO_2 should facilitate excellent cell proliferation compared to an untreated anodized Ti surface, in this manner providing bioactivity to the implant surface and pathways for cell progress at the nanopores via the filopodia.[40]

Further more the results are in Fig. 8. The HOS cells at first attached on M-HAP/TiO_2 (at 80^{o}C) coating and indicated development (growth) to some degree for 1 day (Fig. 8 a). At the point when looking at the development of HOS MG63 cells on M-HAP/TiO_2 coating for 3 days (Fig. 8b), the 7 days cells culture developed more filopodia augmentations (Fig. 8 c).[40] Moreover, besides, the first polygonal shape was kept up which demonstrated that the M-HAP coating gave the vital nutrients supplements to the development (growth) of cells. This indicates that the enhanced cell growth was observed due to the inclusion ratio of minerals in HAP on TiO_2 discussed earlier (Fig. S1). Along these lines, it is declared that the minerals substituted hydroxyapatite coating indicated better biocompatibility without any toxicity.

3.8.3. ALP activity

Cell differentiation was assessed in terms of ALP (alkaline phosphatase) activity of HOS MG63 cells at the end of 1, 3 and 7 days of culture, as shown in Fig. 7. With the increase of culture time, ALP activities increased in HOS MG63 cells on all apatite coatings. The ALP activity of HOS MG63 cells on the M-HAP/TiO_2 (at 80^oC) was significantly higher than that on the M-HAP/Ti (at 80^oC) and HAP/TiO_2 (at 80^oC) coating at, 3 and 7 days. It suggested that the Zn, Mg and Sr substituted HAP nanoparticls coated on TiO_2 surface could enhance the ALP activity of HOS MG63 cells

3.8.4. Filopodia extension

Human osteoblasts (HOS MG63 cells) were cultured on the HAP/TiO_2 (at 80^oC), M-HAP/Ti and M-HAP/TiO_2 (at 80^oC) coatings for 4 h, then cells were fixed, and nuclei were labeled (Fig. 9). Morphology was similar for osteoblasts attached to HAP/TiO_2 and M-HAP/Ti surfaces cells showed long cytoplasmic extensions, filopodia and stress fiber formation (Fig. 9a-c). On the other hand, osteoblasts attached to the M-HAP/TiO_2 (at 80^oC) coatings displayed lamellipodia, finger-like structure and a more diffuse, randomly arranged pattern of cytoplasmic F-actin, with fewer cellular projections.

Interestingly, osteoblast attachment was greater by ~50% on the M-HAP/TiO_2 (at 80^oC) coatings compared to the HAP/TiO_2 surface (Fig. 10a, $p<0.05$). Osteoblast spreading was quantified by measuring the planar area of cells and was found to be similar on each surface, with mean values ranging from 870 to 1050 mm^2 (Fig. 10b, $p>0.05$). In summary, the mineral substituted-HAP/TiO_2 (at 80^oC) coatings influenced osteoblast attachment and focal adhesion formation.

3.8.5. Osteogenic expression

The expression levels of osteogenesis-related genes, including ALP, OCN, OPG, and Col-1, were estimated by the qRTPCR data shown in Fig. 10 (a-d). The addition of minerals induced enhanced gene expression levels. In general, M-HAP/Ti and M-HAP/TiO_2 exhibited higher mRNA levels for all osteogenesis related genes. For each gene, the highest mRNA level was detected on M-HAP/TiO_2 and the lowest on HAP/TiO_2. Therefore, the results of osteoblastic gene expression indicated that the Zn, Mg and Sr in hydroxyapatite coated on TiO_2 were superior to the HAP/TiO_2 coating in supporting MG63 (HOS) cells' differentiation. Previous studies demonstrated that the ionic environment, caused by the dissolution of ions from the biomaterials, has an impact on the biological response of cells.[41,42] Therefore, the substitution of minerals coating sample is much better than those of HAP/TiO_2 coating sample to facilitate cell proliferation and differentiation, and regulates their gene expression on the coating samples.

4. Conclusions

Minerals substituted hydroxyapatite deposition was prosperously developed on anodized TiO_2 substrate by the electrophoretic deposition method. The FTIR, XPS, XRD and SEM results confirmed the formation of M-HAP-coated on anodized titanium. Phase and morphologies for the M-HAP deposits were affected by the deposition temperature. The biofilm conception was restricted by the M-HAP-coatings, which is evidenced by the antimicrobial activity. The M-HAP deposited on TiO_2 surfaces enhanced HOS MG63 cell proliferation compared to untreated Ti surfaces. Thus, the nano-rods, nano-whiskers and nano-flake of M-HAP layers deposited on the anodized Ti had good biocompatibility. Overall, by combing the biocompatibility of M-HAP/TiO_2, the present approach gives an advantageous technique to develop novel implant biomaterials with phenomenal antibacterial properties and great biocompatibility.

Supporting information

The supplementary section contains additional data for Ions released test (Figure. S1**)**, Adhesion strength (Figure. S2**)**, Antimicrobial studies (Figure. S3**),** and preparation of nano M-HAP & HAP (Figure. S4), Protein adsorption (Figure. S5**).**

Acknowledgments

One of the authors, M. Rajan, is grateful to the University Grant Commission (UGC), Government of India, for providing financial assistance under the scheme of "UGC-BSR Research Start-Up Grants" (Ref: No.F.30-21/20014 (BSR). M. Rajan thanks the FIST program for the purchase of a Scanning electron microscopy (SEM) and the University Grants Commission, New Delhi, for funds under UPE programs for the purchase of a high resolution transmission electron microscopy (HRTEM). The authors would like to extend their sincere appreciation to the Deanship of Scientific Research at King Saud University for its funding of this research through the Research Group project No RG-1435-065.

References

1 A. Krza˛kała, A. Kazek-Ke˛sik, W. Simka, **RSC Adv,** 2013, **3**, 19725-19743.

2 H. Schliephake, D. Scharnweber, J. Mater. Chem, 2008, 18, 2404 -2414.

3 W. Simka, A. Krzakała, M. Masełbas, G. Dercz, J. Szade, A. Winiarski, J. Michalska, **RSC Adv**, 2013, 3,11195.

4 M. Ribeiro, F. J. Monteiro, M. P. Ferraz, Biomatter, 2011, 4, 176-194.

5 Y. Li, W. Xiong, C. Zhang, B. Gao, H. Guan, H. Cheng, J. Fu, F. Li, J Biomed Mater Res A, 2014,102, 3939-50.

6 T. Sjöström, L. E . McNamara, L. Yang, M. J. Dalby, Bo Su, Appl. Mater. Interfaces, 2012, 4, 6354-6361.

7 M. Z. Hu, P. Lai, M. S. Bhuiyan, C. T. souris, J. Mater. Sci, 2009, 44, 2820 -2827.

8 Y. Huang, X. Zhang, H. Mao, T. Li, R. Zhao, Y.Yan, X. Pang, RSC Adv, 2015, 5, 17076-17086

9 R. Rodriguez, K. Kim, J. L. Ong, J Biomed Mater Res A, 2003, 65, 352-358.

10 F. Narges, Fahim, T. Sekino, Chem. Mater, 2009, 21,1967 –1979.

11 Q. Wu,C. Liu,L.Fan, J. Shi,H. Jia,Q. Qi,L. Sun, F. Chen, **RSC Adv**, 2013, 3, 7486

12 K. Pal, S. Pal, Materials and Manufacturing Processes, 2006, 21, 325–328.

13 X. Bai, K. More, C. M. Rouleau, A. Rabiei, ActaBiomaterialia, 2010, 6, 2264–2273.

14 H. G. Zhang, Q. Zhu, Y. Wang, Chem. Mater, 2005, 17, 5824-5830.

15 K. Matsunaga, H. Murata, T. Mizoguchi, A. Nakahira, Acta Biomaterialia 2010, 6(6), 2289-2293.

16 R. K. Rude, Journal of Bone, Mineral Research, 1998, 13, 749-758,

17 S. P. Nielsen, Bone, 2004, 35, 583-588.

18 K. Cheng, J. Zhou, W. Weng, S. Zhang, G. Shen, P. Du, Thin Solid Films, 2011, 519, 4647-4651.

19 D. Govindaraj, M. Rajan, M. A. Munusamy, M. D. Balakumaran and P.T. Kalaichelvan, RSC Adv., 2015,5, 44705-44713.

20 ASTM standard F 1044-05. ASTM International, West Conshohocken, PA.

21 L. Zhao, H. Wang, K. Huo, L. Cui, W. Zhang, H. Ni, Y. Zhang, Z. Wu, P.K. Chu. Biomaterials 2011, 32, 5706–5716.

22 D. Wei, R. Zhou, S. Cheng, W. Feng, H. Yang, Q. Du, B. Li, Y. wang, D. Jia, Y. Zhou, J. Mater. Chem . B, 2014, 2, 2993.

23 Q.Yuan, T. D. Golden, Thin Solid Films, 2009, 518, 55.

24 L. Niu, H. Kua, D.H.C. Chua, Langmuir, 2010, 26, 4069-4073.

25 G.H.A. Therese, P.V. Kamath, G.N. Subbann, J Mater Chem, 1998, 8, 405-408.

26 S. Ban , J, Hasegawa, Biomaterials, 2002, 23, 2965–2972.

27. X. Lu, Z. Zhao, Y. Leng, J Crystal Growth, 2005, 284, 506-516.

28 K.P.Musselman, T. Gershon, L. Schmidt-Mende, J. L. MacManus-Driscoll, ElectrochimicaActa, 2011, 56, 3758.

29 N. F. Fahim, T. Sekino, Chem. Mater, 2009, 21,1967.

30 L. Chang, J. Sun, J.Y. H. Fuh ,E. S. Thian, **RSC Adv**, 2013, 3, 11162.

31 X.Lou, D. Barbieri, Y. Zhang, Y. Yan, J. D. Bruijn, H.Yuan, ACS Biomater. Sci. Eng. 2015, 1, 85.

32 S. C. Cox, P. M. Jamshidi, L. Grover, K.K. Mallick, Materials Science and Engineering, 2014,35,106.

33 M. A. Surmeneva, A. Kovtun, A. Peetsch, S. N. Goroja, A. A. Sharonova, V. F. Pichugin,

I. Y. Grubova, A. A. Ivanova, A. D. Teresov, N. N. Koval, V. Buck, A. Wittmar, M. Ulbricht, O. Prymak, M. Epple, R. A. Surmenev, **RSC Adv,** 2013, 3, 11240.

34 W. Xia, C. Lindahl, J. Lausma, P. Borchardt, A. Ballo, P. Thomsen, H. Engqvist, ActaBiomateriali, 2010, 6,1591.

35 E. Milella, F. Cosentino, A. Licciulli, C. Massaro, Biomaterials, 2001, 22, 1425.

36 J. Chen, Y. Song, D. Shan, E. H. Han, Corrosion Science, 2011, 53, 3281.

37 Y. Murakami, K. Sugo, T. Yoshitake, M. Hirano, T. Okuyama, Separation and Purification Technology, 2012, 103, 161.

38 E. Krasicka-Cydzik, K. Kowalski, I. Glazowska, Journal of Achievements in Materials and Manufacturing Engineering, 2006, 18, 147.

39 Y. Wang, j. Tao, Wang, P.T. He and T. Wang, Trans. Nonferrous Met. Soc.China, 2008,18, 631.

40 R. Drevet, A. Viteaux, J. C. Maurin, H. Benhayoune, **RSC Adv**, 2013, 3, 11148.

41 P. Valerio, M. M. Pereira, A. M. Goes and M. F. Leite, Biomaterials, 2004,25, 2941–2948.

42 I. A. Silver, J. Deas and M. Erecinska, Biomaterials, 2001, 22, 175–185.

Figures

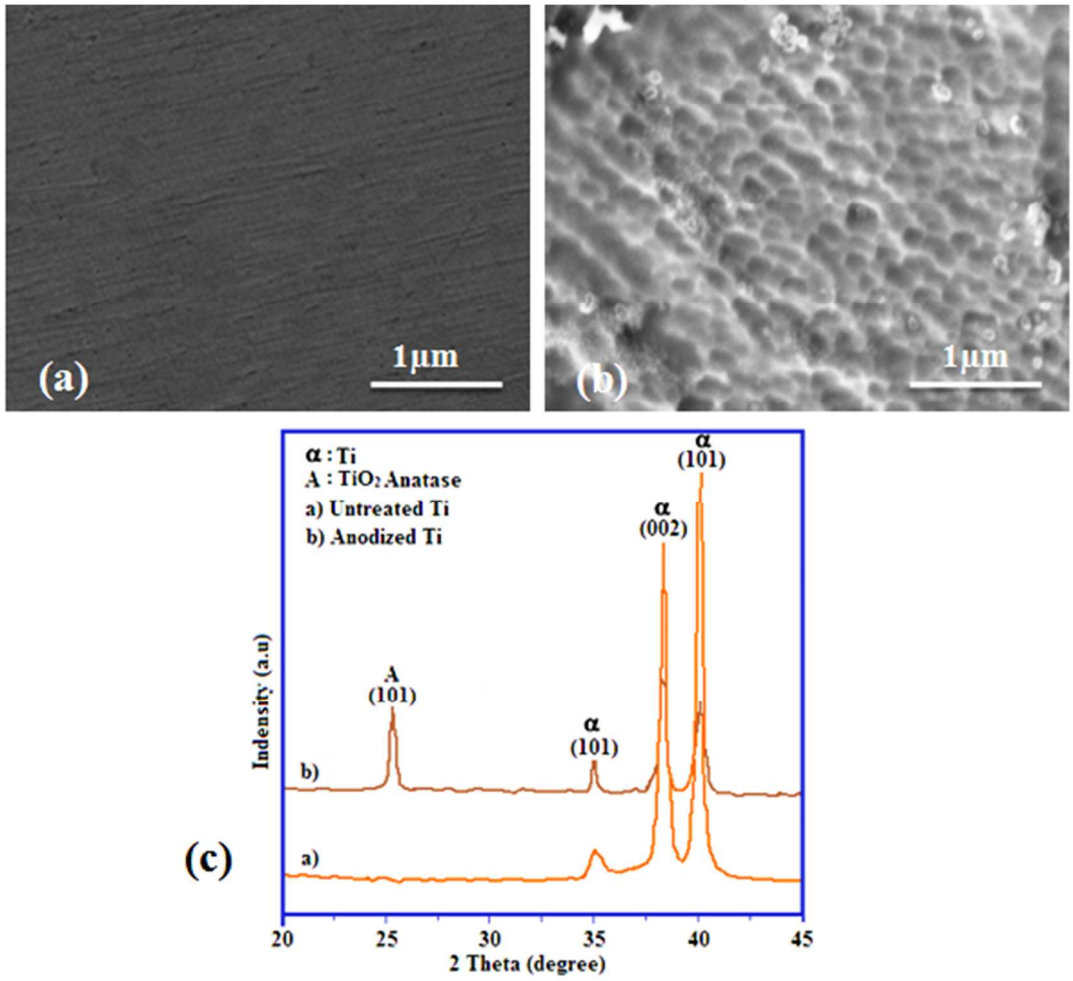

Fig. 1 SEM images of (a) as- received Ti foil (not anodized), (b) anodized foil (TiO_2) and (c) XRD results of both Ti and TiO_2.

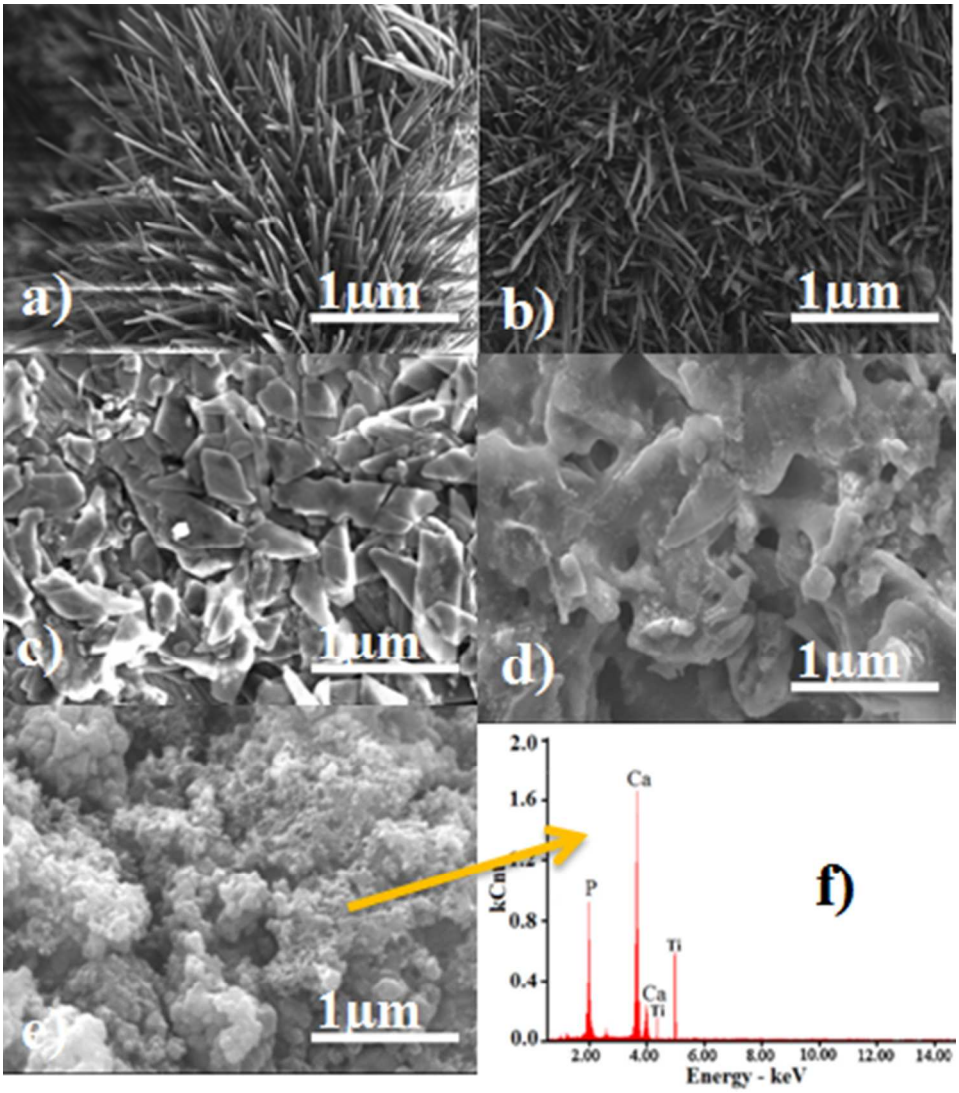

Fig. 2 SEM micrographs of M-HAP deposited on TiO_2 obtained at different deposition temperature: (a) room temperature (b) 60 ^oC (c) 80 ^oC, (d) M-HAP/Ti at 80^oC ,(e) HAP/TiO_2 at 80^oC and (f) elemental composition of HAP/TiO_2 at 80^oC.

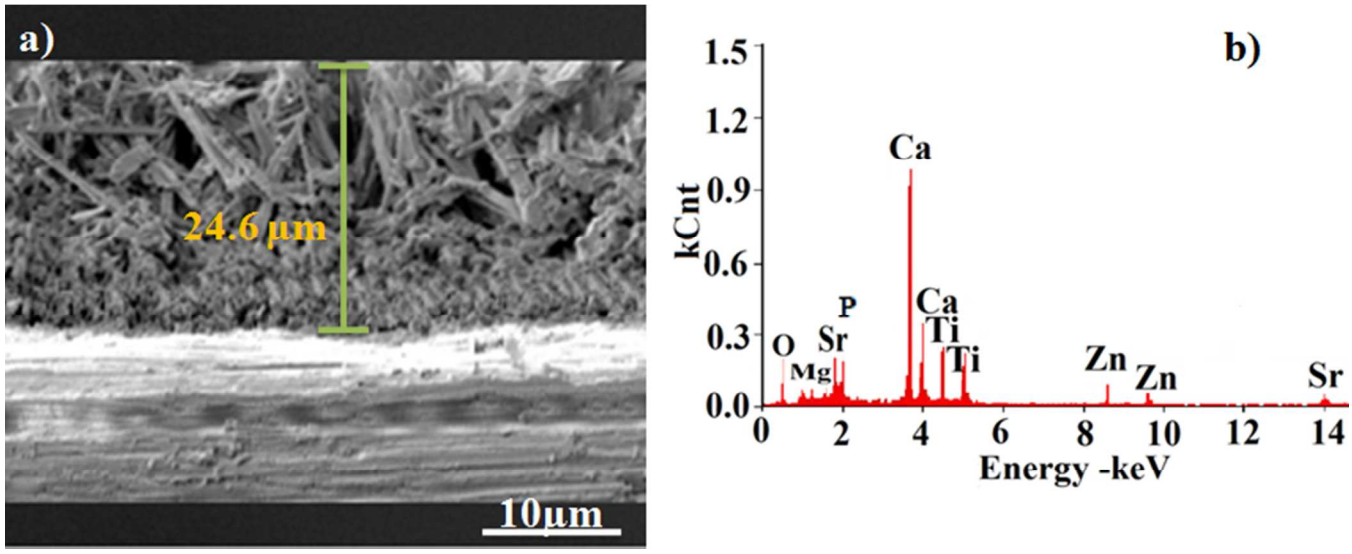

Fig. 3 SEM image of (a) cross-section and (b) EDX spectra of M-HAP coating on TiO_2 at 80°C.

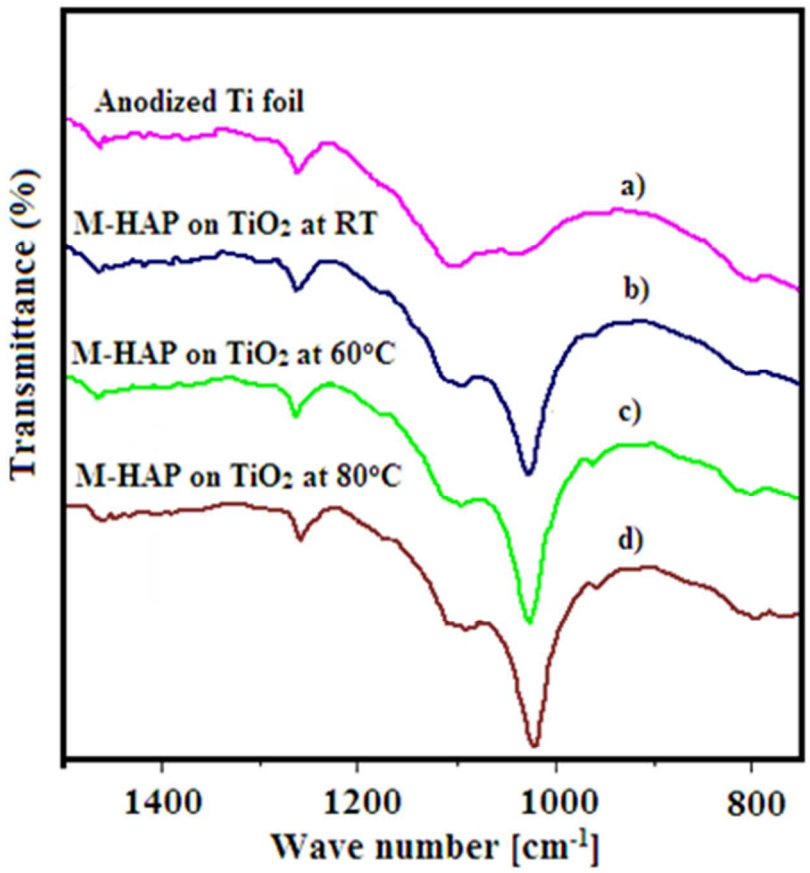

Fig. 4 FTIR spectra of (a) anodized Ti foil, (b) M-HAP deposition at room temperature, (c) M-HAP deposition at 60°C and (d) M-HAP deposition at 80°C.

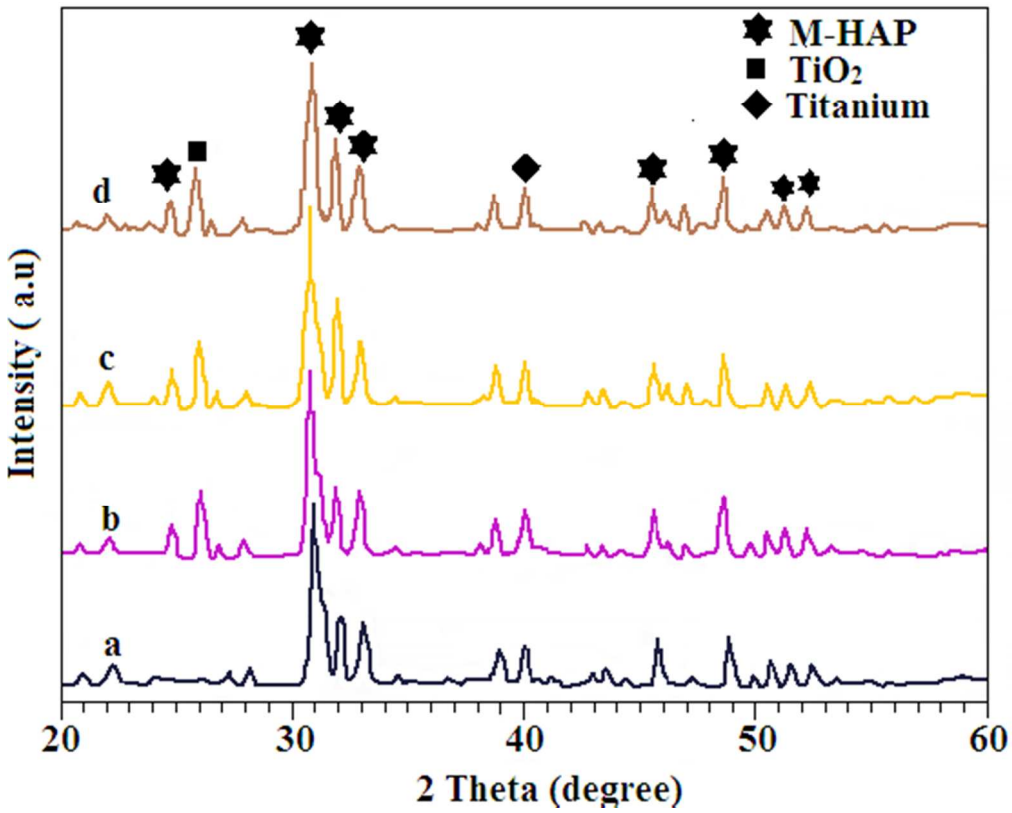

Fig. 5 XRD patterns of M-HAP deposition obtained at different deposition temperature (a) untreated Ti at 80 ^{o}C (b) room temperature (c) 60 ^{o}C and (d) 80 ^{o}C on TiO_2 .

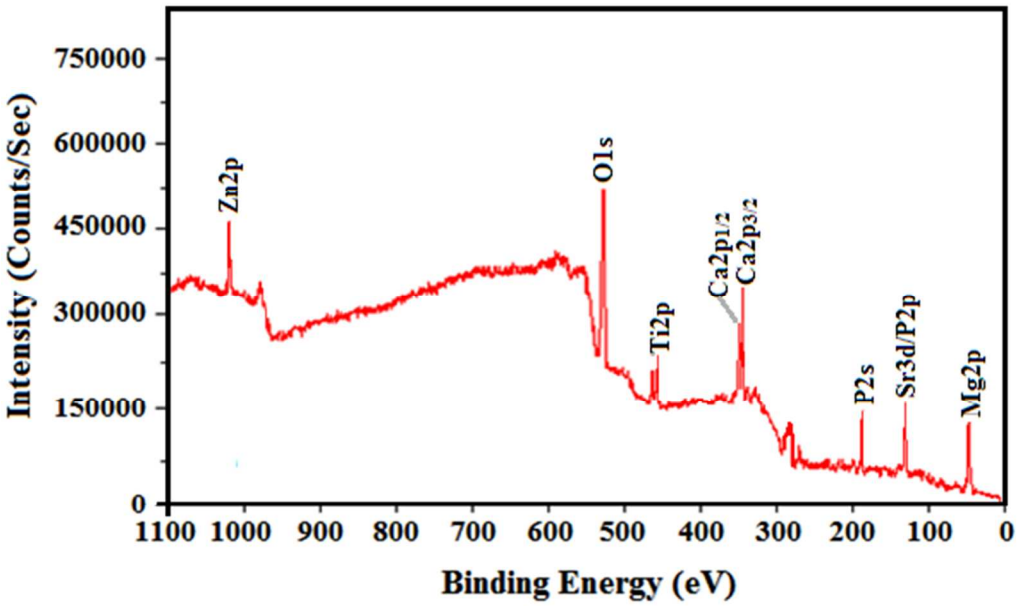

Fig.6 XPS survey spectrum of M-HAP deposited on TiO_2 (at 80^{o}C).

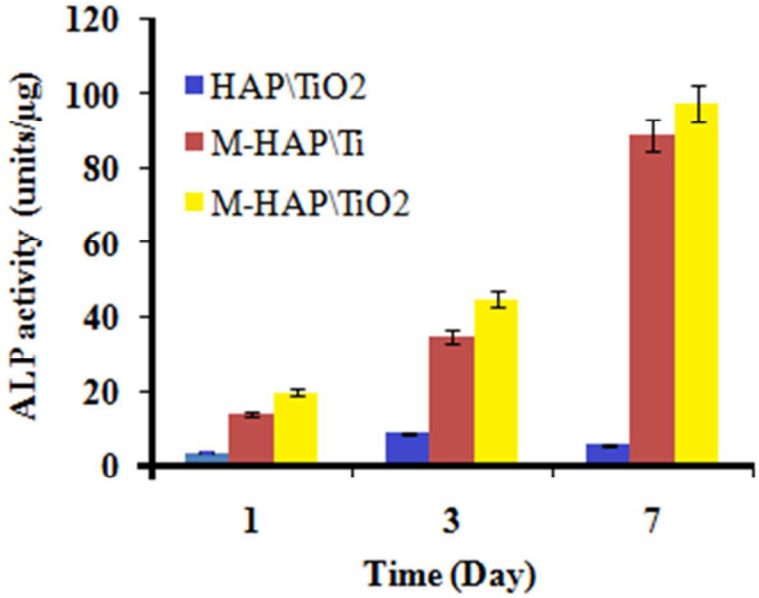

Fig. 7 ALP activity of MG63 (HOS) cells on the HAP/TiO_2, M-HAP/Ti and M-HA/TiO_2 coatings.

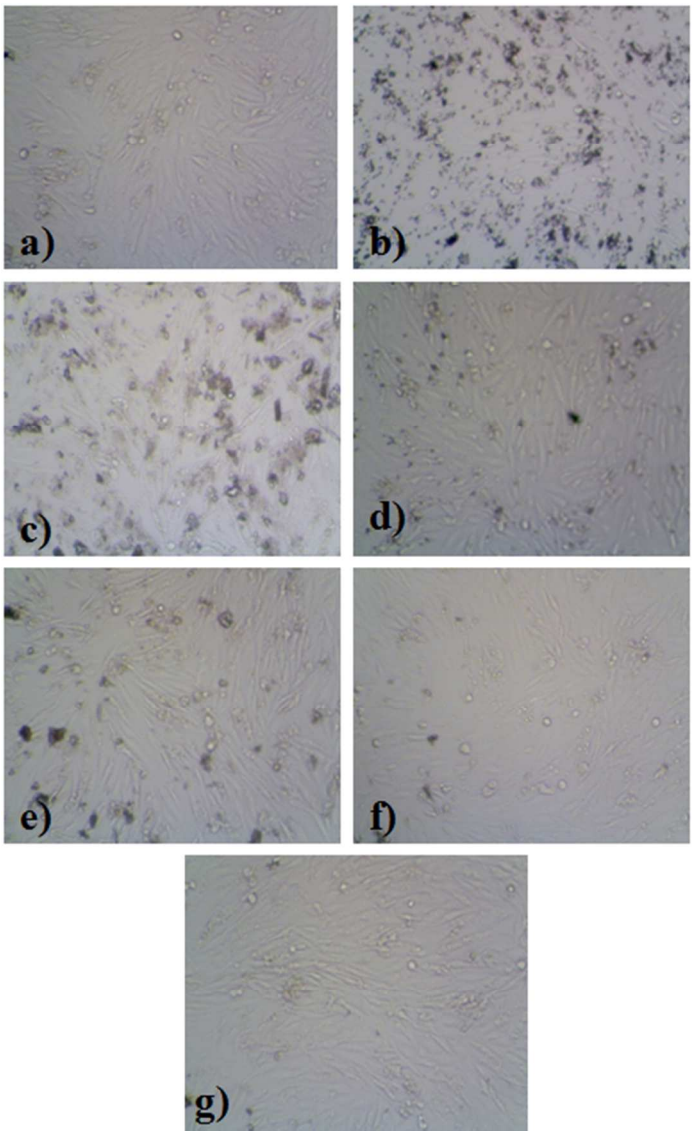

Fig. 8 *In vitro* cytotoxicity of HOS MG63 cells on (a) control, (b) TiO_2, (c) HAP/TiO_2, (d) M- HA/Ti at 80 oC , (e) M-HAP/TiO_2 at RT, (f) M-HAP/TiO2at 60 oC, (g) M-HAP/TiO_2 at 80 ^{o}C.

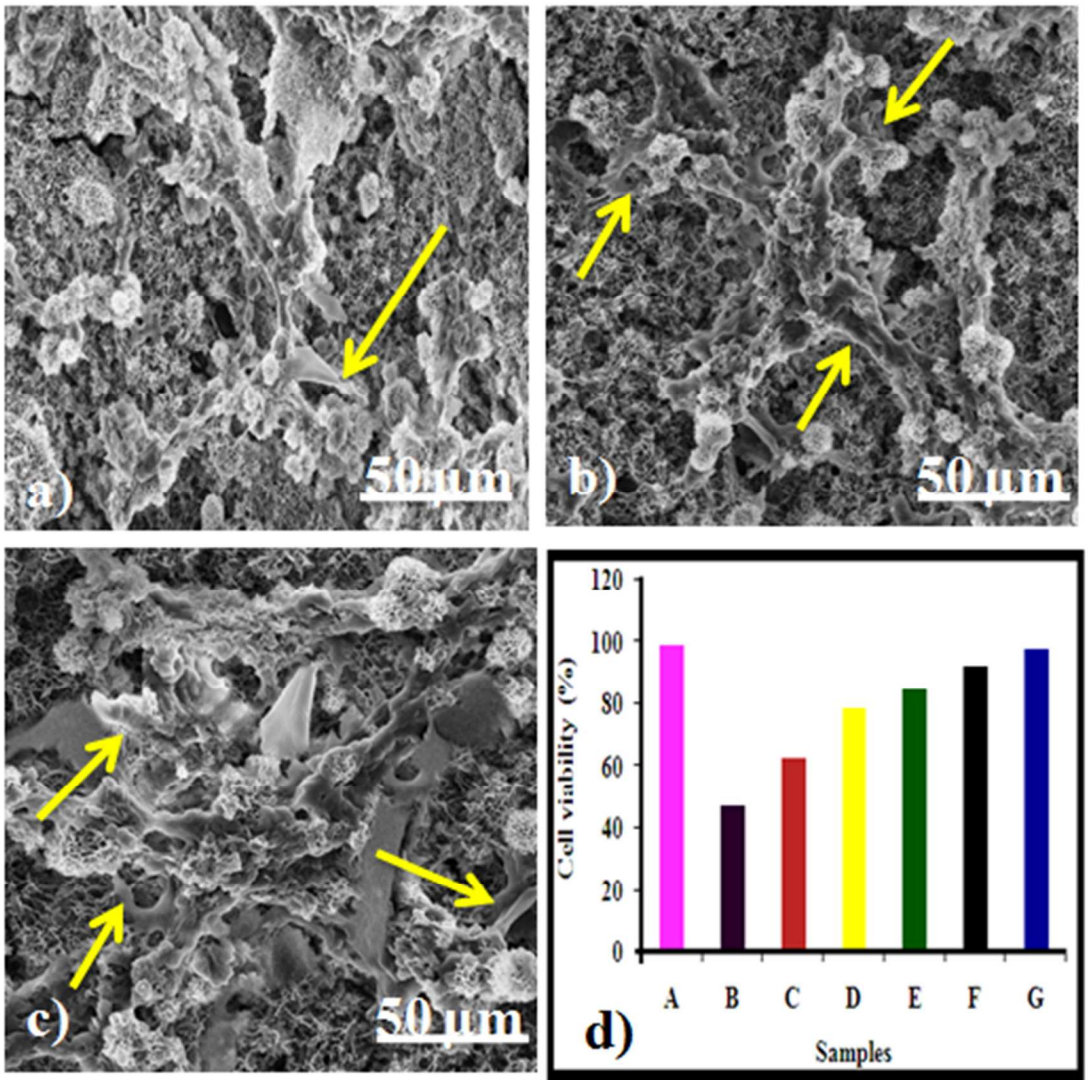

Fig. 9 SEM micrographs illustrating the HOS MG63 cell growth on M-HAP/TiO_2 coating at condition 80^{O}C for the various cultivation time (a) 1 day (b) 3days and (c) 7 days[arrow indication showing cell growth] and (e) Bar diagram showing (A) control, (B) TiO_2, (c) HAP/TiO_2, (C) M-HAP/Ti at 80 ^{o}C, (D) M-HAP/TiO_2 at RT, (E) M-HAP/TiO_2 at 60^{o}C, (F) M-HAP/TiO_2 at 80 ^{o}C.

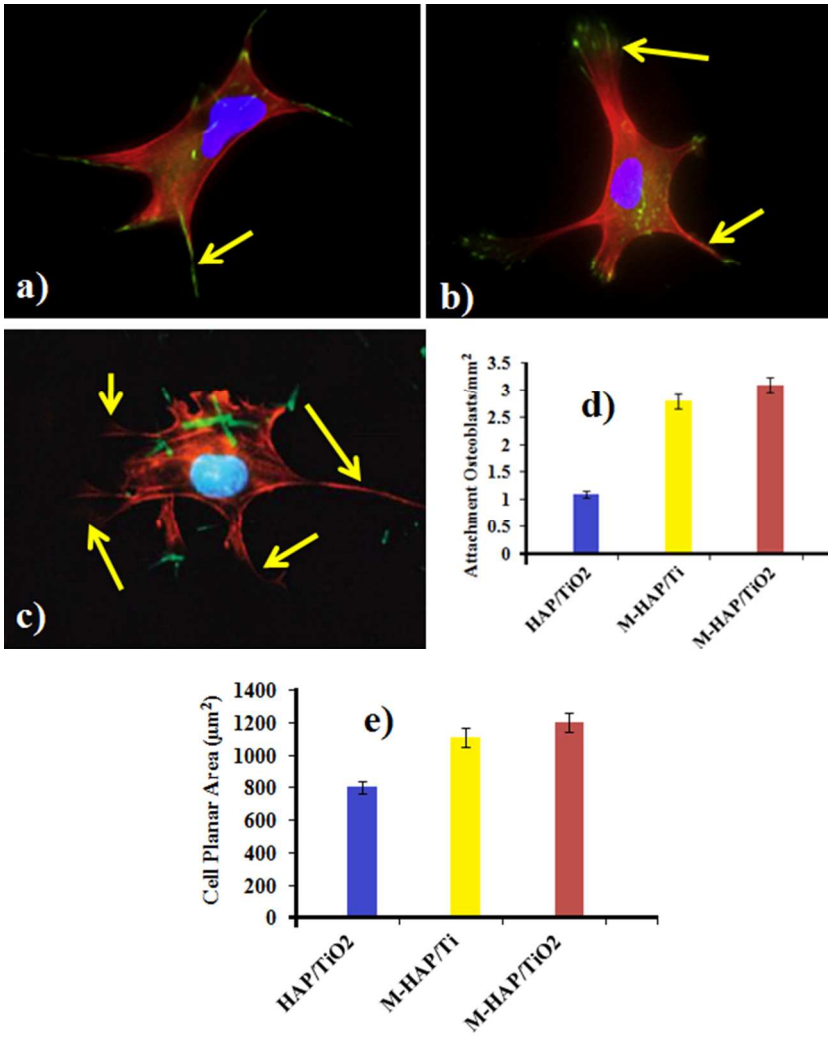

Fig. 10 Effects of minerals substituted HAP surface topography on osteoblast attachment, spreading and focal adhesion formation. Human osteoblasts (HOS) were cultured on the HAP and M-HAP coatings for 4 h. Cells were then fixed, labeled for nuclei (blue), F-actin (red) a) Representative fluorescence images of single osteoblasts on HAP/TiO_2), a) M-HAP/Ti and c) M-HAP/TiO_2 coatings at 80^{o}C. d) Osteoblast attachment was quantified as the number of cells attached per mm^2. e) Cell planar area was quantified by image analysis. Both data are means± SEM of 10 cells per sample with triplicate samples from n=4 independent experiments.

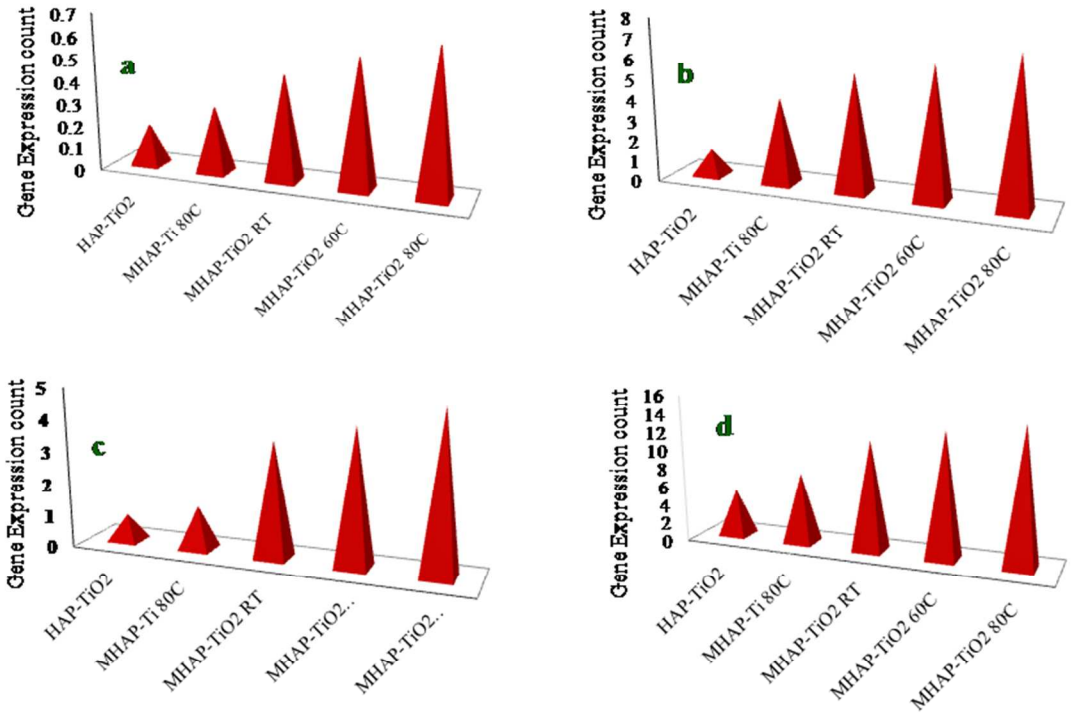

Fig 11 Relative expressions of (a) ALP, (b) OCN, (c) OPG, and (d) Col-1 by MG66 (HOS) cells cultured on different substrates for 2 weeks.

Table1. Primer Sequence

Gene	Forwarded primer sequence (5'–3')	Reverse primer sequence (5'–3')
ALP	GCCTTACCAACTCTTTTGTGCC	CACCCGAGTGGTAGTCACAAT
OCN	CTGACCTCACAGATCCCAAGC	TGGTCTGATAGCTCGTCACAAG
OPG	GGTCAAAGTCTAGGAGTTTCCAG	CACCGCTCTTCATGTGAGAGG
Col-1	GCTCCTCTTAGGGGCCACT	CCACGTCTCACCATTGGGG